Optical properties of a low-temperature bioactive glass powders

Optical properties of a low-temperature bioactive glass powders

U Nurbaiti[1,*], I Rahmawati[1], A Radandima[1], A K Dewi[1], A Yulianto[1], I Sumpono[1] and B Astuti[1]

[1]Department of Physics, Faculty of Mathematics and Natural Sciences, Semarang State University, Indonesia

*Corresponding author: upik_nurbaiti@mail.unnes.ac.id

Abstract. The bioactive glass powders have been synthesis by sol-gel method at low temperature. The silica used as the starting material in this study is silica purified from natural sand with mass variations for amorphous silica and phase variations (Quartz, amorphous). Analysis of the FTIR curves in samples BA1, BA2, BA3 and BQ showed that a lot of group bonds on Bioactive Glass had been formed for all samples. There are Si-O symmetric stretching functional groups (823-825 cm^{-1}), Si-O-Si symmetric stretching functional groups (1047-1050 cm^{-1}), PO4 functional groups (579-606 cm^{-1}), as well as OH symmetry and asymmetry functional groups (3414-3435 cm^{-1}). Meanwhile, the UV-Vis curve reveals the absorption of ultraviolet wavelengths in the range of 230-300 nm for all samples. Although the trend of sample density (BA1, BA2 and BA3) with the SiO_2-amorphous starting material was indicated to decrease with the increase in mass, respectively 0.555 gram/cm^3, 0.553 gram/cm^3 and 0.543 gram/cm^3, the highest density was achieved by the BQ sample of 0.563 gram/cm^3. This density value is still higher than the density of bone tissue so that further synthesis is needed by adding an amorphous SiO_2 starting material.

1. Introduction

There are four different groups of biomaterials as composites, ceramics, polymers and metals. Calcium orthophosphates are widely used [1] since they exhibit non-toxicity and good biocompatibility. However, in acidic environment they have poor mechanical properties and high corrosion rate [2,3], so their use is further restricted as bone implants. Meanwhile, the polymeric biomaterials are widely used for bone tissue applications since they are posses some advantages. Their surface properties and shapes can be easily modified. But, because of some toxic additives such as plasticizers and anti-oxidizers used in synthesis of polymers, their application is limited. Consequently, many studies have been conducted to develop biomaterials by combining the benefit of each group for specific purpose. For example, an Mg-based alloys [4], which is confirmed to have superior mechanical and corrosion performance.

Biocompatible and biodegradable, being pure metals and Mg alloys have been suggested as revolutionary biomaterials to be particularly attractive candidates [1,5]. Their densities are fairly close to each other that remove elastic mismatches between implants and the bone [6,7]. Unfortunately, the fast degradation rates of Mg-based is not match with the kinetics of bone healing, so the necessitates development of implants under controlled degradation rates. A reasonable solution applies the protection to delay the onset of corrosion appears by mixed another biocompatible and biodegradable materials. Calcium orthophosphates are the excellent candidates because they well tolerated by living organisms. This combination causes phenomenon of stress shielding which occurs when the implant

carries higher load [8]. Meanwhile, biomaterial composites are also being widely studied as replacement materials for damaged body parts. Biomaterial composites are able to form a layer of hydroxyapatite on their surface, so they are not rejected by the body [9–12]. Hydroxyapatite is the main mineral phase for bone tissue [13–15], so it is more interesting to study composite as an implant material compared to metal biomaterials. Many research also designed different glass formulations based on the oxide system [16–23] to select the composition. This paper aims to study an optical characteristic on matrix of bioactive glass (BG) for implants base on natural sands as starting materials.

2. Materials and Methods

The natural quartz and amorphous silica powders [24,25] extracted from silica sands were used as raw materials for low-temperature bioactive glass matrix. Some commercial product Merck, i.e., Triethyl phosphate (TEP, $(C_2H_5)_3PO_4$), Calcium nitrate tetrahydrate ($Ca(NO_3)_2.4H_2O$) and Nitric Acid (HNO_3) were also used for produced this matrix by sol-gel method. First, the silica powder was stirred for 45 minutes on the Ethanol (C_2H_5OH) at room temperature. Two droplets of 1M nitric acid were added to hydrolyze the precursor, keep stirring for 45 minutes as well. Then two precursors were added, namely TEP and calcium nitrate tetrahydrate respectively for 1hour of stirring time to obtain a uniform mixture. To remove excess water and ethanol from the mixture, the stirring process is continued by heating at a temperature of 110 °C until a newly gel solution is formed. Finally, the wet gel dried at 250 °C for 3 h. The resulting bioactive glass powders was pulverized in a mortar and sieved, which were used for all characterizations. Functional groups were performed in Perkin Elmer Frontier FTIR spectroscopy data in the range 4000–400 cm−1 of wavenumber, with a KBr as transparent background. Optical measurements were carried out in UV–Vis Shimadzu spectrophotometer spectra to determine the transmittance and absorbance spectra in the range of 200–1100 nm wavelength. The bulk densities of the samples were obtained according to the Archimedes principle.

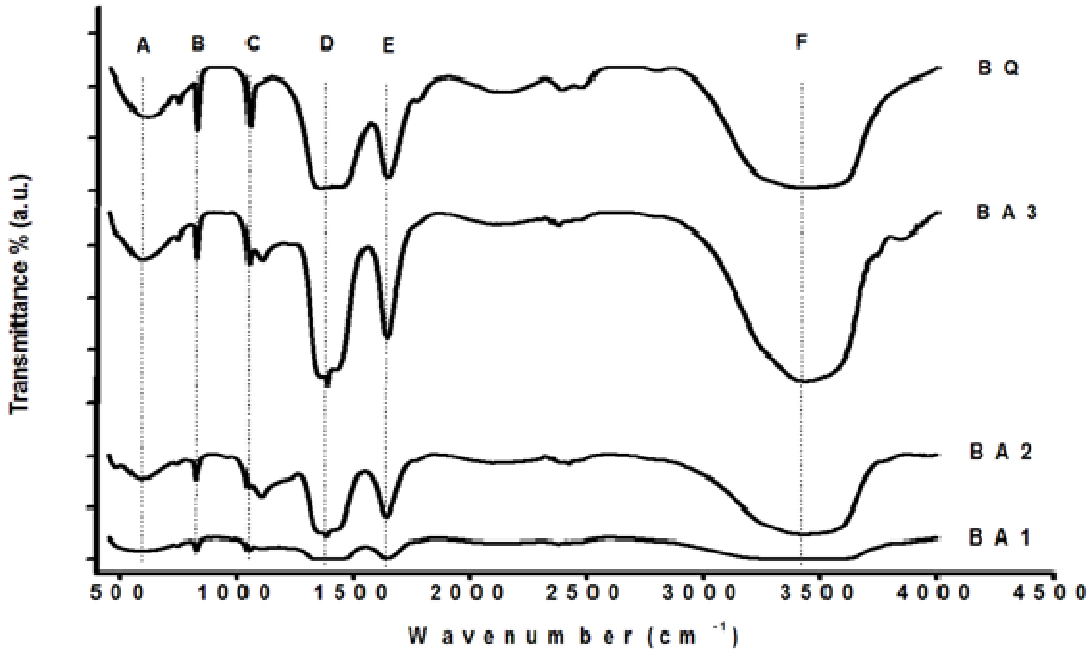

Figure 1. FTIR pattern of the samples (BA1, BA2, BA3 and BQ) at room temperature.

Table 1. Position of the functional groups present in the sample.

Functional Structure	Wavenumber (cm^{-1})				Reference
	BA1	BA2	BA3	BQ	
O-H symmetric stretching	3414.00	3429.45	3434.90	3435.40	[27]
O-H bending vibration	1638.02	1640.05	1638.03	1635.00	[26]
-CH_3 symmetric bending	1430.04	1425.10	1420.08	1425.09	[15]
Si-O-Si asymmetric stretching	1047.91	1049.52	1048.34	1047.53	[16]
Si-O-Si bending vibration	823.96	824.89	824.90	823.02	[28]
-PO_4^{3-} asymmetric bending	579.13	587.98	592.08	606.09	[19]

3. Results and Discussion

The FTIR spectra of all BG's samples are shown in Figure 1. There aren't differences in the peaks of vibration for all samples, so it can be understand that the samples have the same chemical bonding structures. FTIR spectra as shown in the fig.1 revealed characteristic peaks attributed some absorption bands of samples. The absorption band at E (~1630 cm^{-1}) and F (~3400 cm^{-1}) peaks were assigned to vibration modes of H_2O [27], which band was ascribed to the bending vibration and symmetric stretching modes of O-H groups, respectively. The presence of O-H groups in all samples indicates that the sample is hygroscopic nature so it tends to absorb H_2O easily. Furthermore, the sharp peak at D (band between 1400 and 1460 cm^{-1}) was observed due to the appearance of $–CH_3$ groups [15], which is associated with scissoring of $–CH_2$ by ethanol as a solvent. Meanwhile, the broad vibration bands at around 1040 cm^{-1} (C peak) and 870 cm^{-1} (B peak) were ascribed asymmetric stretching and bending vibration to the Si-O-Si, respectively. On the other hand, the phosphorus in the form of orthophosphate (PO_4^{3-}), whose charge is balanced by modifier Ca^{2+} was confirmed by the asymmetric bending of PO_4^{3-} at peak A 570 cm^{-1}[18–20]. Most of bands appeared on the same position, it was indicated that the glass has same as nucleation structure. Although the intensities of some bands increased with the increase in the SiO_2 content, as shown in Figure 1, BA1, BA2 and BA3, the intensity also rose for the other one phase, i.e., quartz as shown in Figure 1 BQ. The quantity of peak group bond values in this study for all samples is shown in Table 1.

Table 2. Density and energy gab of the samples

Sample	**Si** (mol)	**P/Si** (%)	**Density** ($gram/cm^3$)	**Eg** (eV)
BA1	0.62	14.60	0.555	3.94
BA2	1.23	7.32	0.553	3.99
BA3	2.43	3.66	0.543	3.91
BQ	0.62	14.60	0.563	3.99

Figure 2 shows the UV-VIS absorption spectra recorded at room temperature for samples in the wavelength range 200-1100 nm. From this figure, it can be seen that all samples (BA1, BA2, BA3 and BQ) reveal no absorption peaks in the visible region, but two absorption peaks were observed in the ultraviolet region. The first peak was observed at about 240-246 nm for all samples, and at peak 275-280 nm for the second one. A small shift to longer wavelength at the position of this absorption band was observed with the increase in the Si_2O-amorphous mass content. A small shift also occurred in the BQ sample which had a different phase but still had the same mass content as BA1 sample, this shift

phenomenon was also observed by previous researchers [8]. The intensity of peak was detected to decrease with rising of Si_2O-amorphous mass content, as well as samples with different Si_2O-quartz phases. A significant decrease in the intensity of the quartz phase is suspected to be closely related to the crystalline structure. This assumption is supported by the density measurement results. From Table 2, it is found that the BQ sample has the highest density (0.563 gram/cm^3).

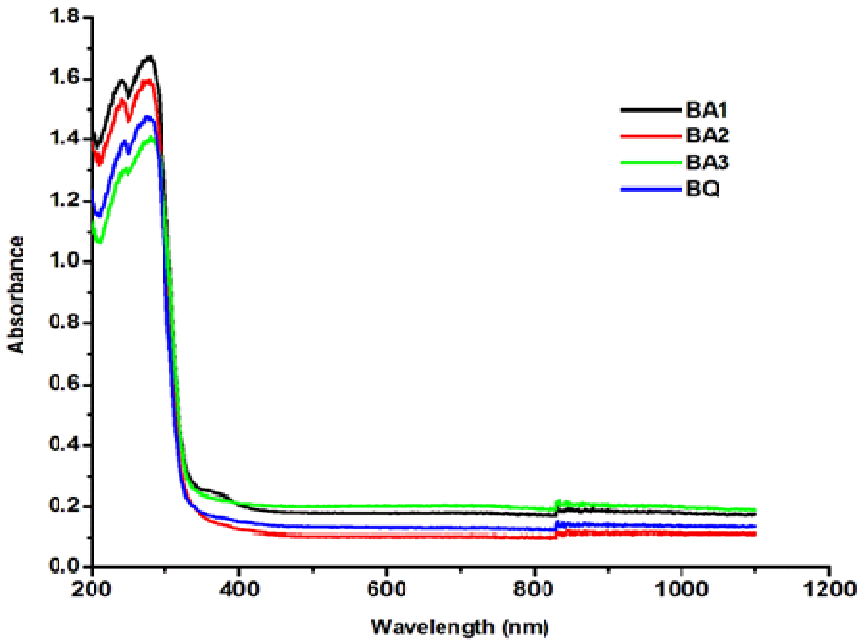

Figure 2. UV-VIS pattern of the samples (BA1, BA2, BA3 and BQ) at room temperature.

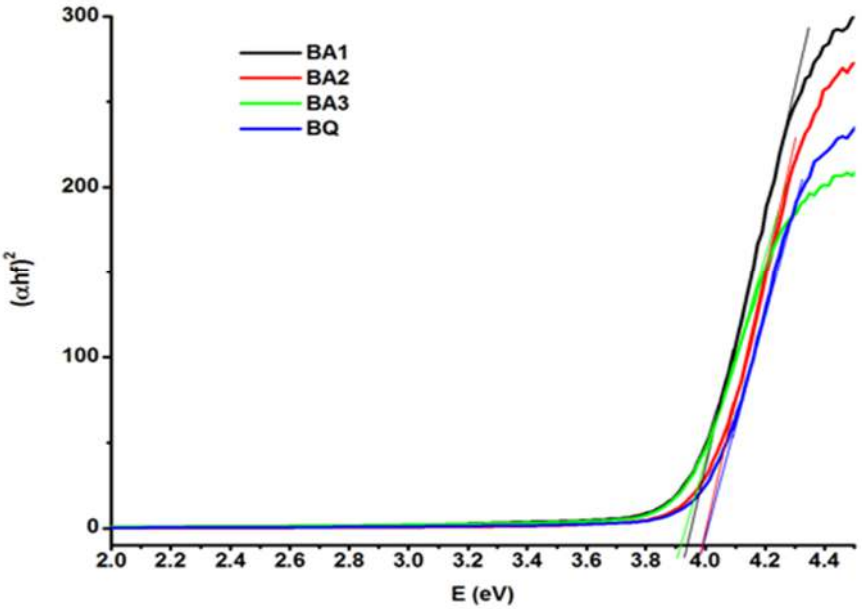

Figure 3. Tauc's plot $(\alpha hf)^2$ versus E(eV).

The absorbing molecules in Figure 2 show the effect of the mass amount of amorphous silica in the bioactive glass BA1, BA2 and BA3, while the effect of the phase difference is denoted by BQ. In order to obtain further insight of the investigated bioactive glass samples, UV-Vis energy spectra were calculated. The band gap energy of the sample is determined by extrapolating the linear part of the graph in Figure 3. Thus, the band gap energy is obtained from the straight-line intersection between the curve $(\alpha hf)^2$ to the photon energy (E) on the x-axis [29]. The values of energy band gap generated from these samples were around between 3.91 to 3.99 eV for all samples, Table 2.

4. Conclusion

The low-temperature bioactive glasses powders briefly synthesized for biomedical products by used natural silica sands. The similar FTIR spectral patterns of the various samples indicate that the composition of the group bonds is identical for all glass bioactive matrices. Meanwhile, the UV-Vis spectrum pattern with the same peaks shows that the energy is absorbed in the wavelength band. The value of gab energy in the range between 3.91-3.99 eV obtained by extrapolating the absorbance curve makes this matrix categorized as an insulating material.

Acknowledgments

The research was supported by Grand of DIPA (Daftar Isian Pelaksanaan Anggaran) 2020 Faculty of Mathematics and Natural Science Universitas Negeri Semarang decentralization scheme by contract number: 72.28.5/UN37/PPK.4.4/2020.

References

[1] Dorozhkin S V 2014 *Acta Biomater.* **10**(7) 2919
[2] Sezer N, Evis Z, Kayhan S M, Tahmasebifar A, and Koç M 2018 *J. Magnes. Alloys* **6**(1) 23
[3] Tahmasebifar A, Kayhan S M, Evis Z, Tezcaner A, Çinici H, and Koç M 2016 *J. Alloys Compd.* **687** 906
[4] Chen Y, Xu Z, Smith C, and Sankar J 2014 *Acta Biomater* **10**(11) 4561
[5] Cheng J, Liu B, Wu Y H, and Zheng Y F 2013 *J. Mater. Sci. Technol.* **29**(7) 619
[6] Li J, Tan L, Wan P, Yu X, and Yang K 2015 *Mater. Sci. Eng.: C* **49** 422
[7] A B, J W, Ma G, and C W 2012 *Acta Biomater* **8**(5) 1661
[8] Ahmed A A, Ali A A, Mahmoud D A R, and El-Fiqi A M 2011 *Solid State Sci.* **13**(5) 981
[9] Rahaman M N, Xiao W, and Huang W 2018 *Bioact. Glas.* 285
[10] deOliveira A A R, deSouza D A, Dias L L S, deCarvalho S M, Mansur H S, and Pereira M de M 2013 *Biomed. Mater.* **8**(2) 025011
[11] Ravarian R, Moztarzadeh F, Hashjin M S, Rabiee S M, Khoshakhlagh P, and Tahriri M 2010 *Ceram. Int.* **36**(1) 291
[12] Hench L L 2006 *J Mater Sci: Mater Med* **17**(11) 967
[13] Kamalian R, Yazdanpanah A, Moztarzadeh F, Ravarian R, Moztarzadeh Z, Tahmasbi M, and Mozafar M 2012 *Ceram.-Silik.* **56**(4) 331
[14] Bellucci D, Sola A, Salvatori R, Anesi A, Chiarini L, and Cannillo V 2014 *Mater. Sci. Eng.: C* **43** 573
[15] Bellucci D, Antonella Sola, Gazzarri M, Chiellini F, and Cannillo V 2013 *Mater. Sci. Eng.: C* **33** 1091
[16] Cacciotti I, Lombardi M, Bianco A, Ravaglioli A, and Montanaro L 2012 *J Mater Sci: Mater Med* **23**(8) 1849
[17] Bellucci D, Cannillo V, and Sola A 2010 *Mater. Lett.* **64**(2) 203
[18] Altomare L, Bellucci D, Bolelli G, Bonferroni B, Cannillo V, Nardo L D, Gadow R, Killinger A, Lusvarghi L, Sola A, and Stiegler N 2011 *J Mater Sci: Mater Med* **22**(5) 1303
[19] Sola A, Bellucci D, Raucci M G, Zeppetelli S, Ambrosio L, and Cannillo V 2012 *J. Biomed. Mater. Res. A* **100**(2) 305
[20] Chen Q-Z and Thouas G A 2011 *Acta Biomater* **7**(10) 3616
[21] Jones J R, Brauer D S, Hupa L, and Greenspan D C 2016 *Int. J. Appl. Glass Sci.* **7**(4) 423

[22] Bellucci D, Sola A, and Cannillo V 2013 *Mater. Sci. Eng.: C* **33**(4) 2138
[23] Pelaseyed S S, MadaahHosseini H, and Samadikuchaksaraei A 2020 *J. Biomed. Mater. Res. A* **108**(6) 1390
[24] Pratapa S, Handoko W D, Nurbaiti U, and Mashuri 2017 *Ceram. Int.* **43**(9) 7172
[25] Nurbaiti U, Triwikantoro, Zainuri M, and Pratapa S 2016 *AIP Conference Proceedings* **1725** 020056
[26] Suzuki C K, Santos M F M, Ono E, Fujiwara E, Torikai D, and Shinohara A H 2012 Strategic High Quality Quartz Supply for Fusion into Silica Glass *Processing, Properties, and Applications of Glass and Optical Materials* (John Wiley & Sons, Ltd) pp 69–74
[27] Goh Y-F, Alshemary A Z, Akram M, Kadir M R A, and Hussain R 2014 *Int. J. Appl. Glass Sci.* **5**(3) 255
[28] Bui X V and Dang T H 2019 *Process. Appl. Ceram.* **13**(1) 98
[29] Kärber E, Katerski A, Acik I O, Mere A, Mikli V, and Krunks M 2016 *Beilstein J. Nanotechnol.* **7**(1) 1662